

Termination of Graphene Edges Created by Hydrogen and Deuterium Plasmas

Taisuke Ochi,^{*} Masahiro Kamada, Takamoto Yokosawa,
Kozo Mukai¹, Jun Yoshinobu¹, and Tomohiro Matsui[†]

*Advanced Research Laboratory, Anritsu Corporation,
5-1-1, Onna, Atsugi, Kanagawa 243-8555, Japan and*

¹*The Institute for Solid State Physics, The University of Tokyo,
5-1-5, Kashiwanoha, Kashiwa, Chiba, 277-8581, Japan*

Edge engineering is important for both fundamental research and applications as the device size decreases to nanometer scale. This is especially the case for graphene because a graphene edge shows totally different electronic properties depending on the atomic structure and the termination. It has recently been shown that an atomically precise zigzag edge can be obtained by etching graphene and graphite using hydrogen (H) plasma. However, edge termination had not been studied directly. In this study, termination of edges created by H-plasma is studied by high-resolution electron energy loss spectroscopy to show that the edge is sp^2 bonded and the edge carbon atom is terminated by only one H atom. This suggests that an ideal zigzag edge, which is not only atomically precise but also sp^2 bonding, can be obtained by H-plasma etching. Etching of the graphite surface with plasma of a different isotope, deuterium (D), is also studied by scanning tunneling microscopy to show that D-plasma anisotropically etches graphite less efficiently, although it can make defects more efficiently, than H-plasma.

Keywords: Graphene; Hydrogen plasma etching; High resolution electron energy loss spectroscopy;

1. INTRODUCTION

Graphene, a two-dimensional sheet of carbon (C) atoms, is attracting vast interest and its bulk properties have been studied extensively since its discovery [1–10]. One of the still-remaining frontiers of graphene research resides in its edges. Among two types of graphene edge structures, i.e., zigzag and armchair, the biparticle symmetry is broken along the zigzag edge. As a result, a flat band is expected to appear at the Fermi energy (E_F) around the K point. Interestingly, this flat band can split due to spin polarization under electron-electron interaction, similarly to flat-band ferromagnetism [11]. Experimentally, the spin-unpolarized zigzag edge state has been observed on graphite surfaces by scanning tunneling microscopy and spectroscopy (STM/S) as a peak in the local density of state (LDOS) at around E_F , which is spatially localized only around the zigzag edge [12–14]. However, further study of the zigzag edge state including the spin-polarized state is limited because it is difficult to prepare a zigzag edge that is comparable to theoretical models. Namely, the zigzag edge should be atomically precise and, at the same time, it should be terminated by only one

hydrogen (H) atom to preserve sp^2 bonding of the honeycomb lattice along the edge.

Recently, it has been found that hexagonal nanopits with atomically precise zigzag edges can be prepared on graphene and graphite surfaces by exposing them to remote H-plasma at high temperatures [15–19]. Figure 1(a) illustrates a typical surface structure of graphite etched by H-plasma. Even a LDOS suggestive of the spin-polarized state was observed for graphene nanoribbons terminated by parallel zigzag edges (z-GNRs) prepared using this H-plasma etching (HPE) technique. However, termination of the edge is still unclear. Considering that the edges are prepared by a chemical reaction with H, the edge C atoms are most probably terminated by H. But the chemical bonding of the edge is not trivial. It can be sp^2 bonded if the edge C atom is terminated by one H atom as illustrated in Figure 1(b), otherwise, it is sp^3 bonded if the edge C atom is terminated by two H atoms as shown in Figure 1(c). Although an analysis of STM images together with a consideration of the chemical potential suggests that the edge is sp^2 bonded and terminated by one H atom [20], there are no direct observations that show edge termination unambiguously.

Edge termination of graphene nanoislands on Pt(100) and Pt(111) has been studied by high-resolution electron energy loss spectroscopy

^{*}Corresponding author: Taisuke.Ochi@anritsu.com

[†]Corresponding author: Tomohiro.Matsui@anritsu.com

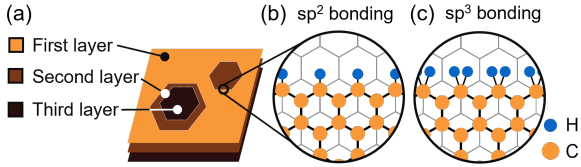


Figure 1: (a) Illustration of a typical surface structure prepared by H- and D-plasma etching. Some hexagonal nanopyts are created layer by layer. Atomic configuration of (b) sp^2 - and (c) sp^3 -bonded zigzag edges. The edge C atom is terminated by one (two) H atom(s) for the sp^2 (sp^3)-bonded edge. The hexagonal lattice of the second layer is also shown.

(HREELS) [21, 22]. In these studies, nanoislands were prepared by thermal decomposition of hydrocarbons, and their edges were terminated by either H or deuterium (D) by exposing the nanoislands to thermally dissociated H or D. They showed both stretching and bending modes of C-H (ν_{CH} and δ_{CH}) and C-D (ν_{CD} and δ_{CD}) clearly as isolated peaks in the spectra. Edge termination was determined by comparing these stretching modes with those measured for submonolayer benzene and cyclohexane adsorbed on Pt(111) [23, 24]. Note here that benzene is composed of sp^2 -bonded C atoms, while cyclohexane is composed of sp^3 -bonded C atoms. It was concluded that the edges of graphene nanoislands were sp^3 bonded and terminated by two H or D atoms, because the energies of the stretching modes were closer to those for cyclohexane than those for benzene.

Theoretically, on the other hand, the local vibrational density of states were calculated for GNRs with both zigzag and armchair edges terminated by only one H atoms, namely sp^2 -bonded edges [25, 26]. They showed an isolated peak at around 2900 cm^{-1} and a bunch of peaks at lower energies than 1800 cm^{-1} . The authors suggested that the isolated peak at higher energy originated from the ν_{CH} at the edge, while the peaks at lower energies include edge-localized phonon modes and surface phonon modes.

In this work, termination of the edges created by the H- and D-plasma etching of graphite was studied by HREELS. In contrast to the nanoislands on Pt surfaces studied previously [21, 22], our samples were graphene nanopyts on graphite surfaces. The ν_{CH} and the ν_{CD} were observed as isolated peaks at around 2890 cm^{-1} and 2143 cm^{-1} , respectively, suggesting that the edges prepared by HPE of graphite is sp^2 bonded and terminated by only one H atom. In

addition, it is also suggested that edge termination is robust even under ambient conditions. Besides the HREELS study, the similarities and the differences between the etching by H- and D-plasma were also studied by STM.

2. EXPERIMENTAL

The H- and D-plasma etched samples (HPE and DPE samples) were transferred from the etching chamber to the ultra-high vacuum (UHV) chamber for HREELS within several hours. To eliminate unknown effects occurring by exposing the sample to the atmosphere, the edge of the DPE sample re-terminated by either H or D atoms in-situ in the UHV chamber (H- or D-modified sample) was also studied. Here, the edge termination of the DPE sample was first removed by heating the sample up to $T \sim 1000\text{ K}$ for 5 minutes (cleaned sample), and it was then exposed to H or D atoms, which were thermally dissociated from either H_2 or D_2 by a tungsten (W) filament (ϕ 0.3 mm) at $T \sim 1700\text{ K}$ located about 10 cm away from the sample surface for 1 to 2 hours. During this dissociation and re-termination process, the sample was cooled at $T \sim 100\text{ K}$ under H_2 or D_2 pressure of $5.0 \times 10^{-6}\text{ Pa}$. It was confirmed by STM that the surface structure was not changed by this procedure after the HREELS measurement. Note that all the samples were baked at $400\text{--}600\text{ K}$ before the HREELS measurement to remove physisorbed species on the sample surface.

The HREELS measurements were performed for graphite ($\sim 12\text{ mm} \times 12\text{ mm} \times 1\text{ mm}$) rather than graphene to obtain sufficient signal from the edge. The parameters for the H- and D-plasma etching were tuned to obtain as many hexagonal nanopyts as possible. By calculating the edge length from the STM images, one can expect that around 5.9×10^4 and 8.4×10^4 edge atoms/ μm^2 were prepared for the HPE and DPE samples, respectively, which is sufficient to obtain C-H and C-D vibrational signals by HREELS (ELS5000, LK Technologies).

The HREELS spectra were obtained at $T \sim 90\text{ K}$ with a primary electron energy of 7 eV and an incident angle of 60° from the sample normal. The energy resolution was 48 cm^{-1} (6 meV) in a specular detection geometry. The measurements were performed in an off-specular geometry, where the detection angle from the sample normal was 50° for the HPE, DPE and D-modified samples, while it was 45° for the H-modified and cleaned samples. This

difference in detection angle only affects the background intensity, and the C-H and C-D vibration signals are barely affected.

On the other hand, all STM images were obtained in constant current mode ($I = 1.0$ nA, $V = 500$ mV) under atmospheric conditions.

3. RESULTS AND DISCUSSION

3.1. Etching behavior of D-plasma

First of all, the etching behavior of the D-plasma for the graphite surface was investigated. Figure 2(a, b) shows the STM images of graphite surfaces etched by H- and D-plasma, respectively, with the same etching parameters. For both samples, hexagonal nanopits are created and the etching behaviors are similar to each other. This suggests that the chemical reaction of H- and D-plasma etching for graphite is identical. However, the details are different. For example, D-plasma etches the graphite surface more deeply than the H-plasma. The difference is quantitatively analyzed by calculating the area fraction of the n -th layer from the surface (S_n) and the maximum nanopit size of the first layer (D_{\max}) as shown in Figure 2(c, d), respectively. The definitions of S_n and D_{\max} follow Reference [18]. Figure 2(c) clearly suggests that the larger surface area is etched away and that deeper layers appear by D-plasma etching than by H-plasma etching. On the other hand, the D_{\max} of the D-plasma etched sample is smaller just slightly than that of the H-plasma etched one as shown in Figure 2(d). Considering that H-ions, such as H^+ , H_2^+ , H_3^+ , create surface defects and that H-radicals enlarge the defects into nanopits in HPE [17–19], the difference between H- and D-plasma etching suggests that D-ions create surface defects more efficiently than H-ions, while the effect of enlarging the defects by D-radicals is similar to or weaker than that by H-radicals, at least under these etching conditions.

3.2. HREELS measurement

Figure 3 shows the HREELS spectra for the HPE, DPE, H-modified, D-modified and cleaned samples. Several electron energy loss peaks are observed for all the samples except the cleaned one. For the HPE, DPE and H-modified samples, two spectra are overlaid, i.e., one with a wide energy range but with low

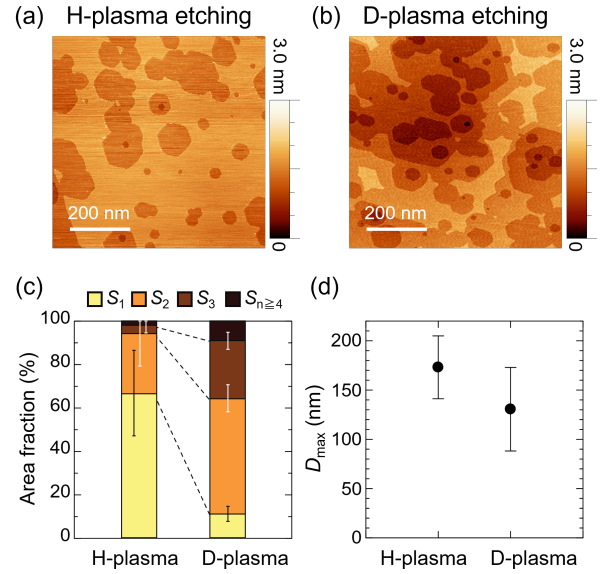


Figure 2: Comparison between H-plasma and D-plasma etchings. (a) and (b) are STM images of graphite surfaces etched by H-plasma and D-plasma, respectively, with the same etching parameters. (c) and (d) are S_n and D_{\max} extracted from the STM images, respectively.

energy resolution depicted by a light color and the other with narrow energy range but with high energy resolution depicted by a dark color. Only for the HPE sample, peaks appear at around 720 cm^{-1} and 3360 cm^{-1} , the intensities of which change time by time. They originate from the vibrational modes of H_2O , namely the frustrated rotation (or libration) mode of H_2O (ν_{RH_2O}) and the O-H stretching mode (ν_{SH_2O}), respectively [27], due to the adsorption of water in the UHV chamber at low temperatures. Note that such effect does not appear for the other samples. For the cleaned sample, on the other hand, only energy losses related to the surface phonons of in-plane transverse acoustic (TA) mode at around 110 cm^{-1} and in-plane transverse optical (TO) and longitudinal optical (LO) modes at around 1580 cm^{-1} [28, 29] are observed. This indicates that the edge terminations are certainly removed by heating at $T \sim 1000$ K.

For the samples other than the cleaned one, a bunch of peaks including bending mode and edge-localized phonon mode are observed at wave numbers lower than 1600 cm^{-1} . The spectra are too complicated to identify each peak and its origin. On the other hand, an isolated peak is observed at energies higher than 2000 cm^{-1} for all the samples except the cleaned one. If the peaks are fitted by single gaussian, the peak positions for the HPE, DPE, H-modified and D-modified samples are at 2901 , 2884 , 2876 and 2902 cm^{-1} , respectively. For the

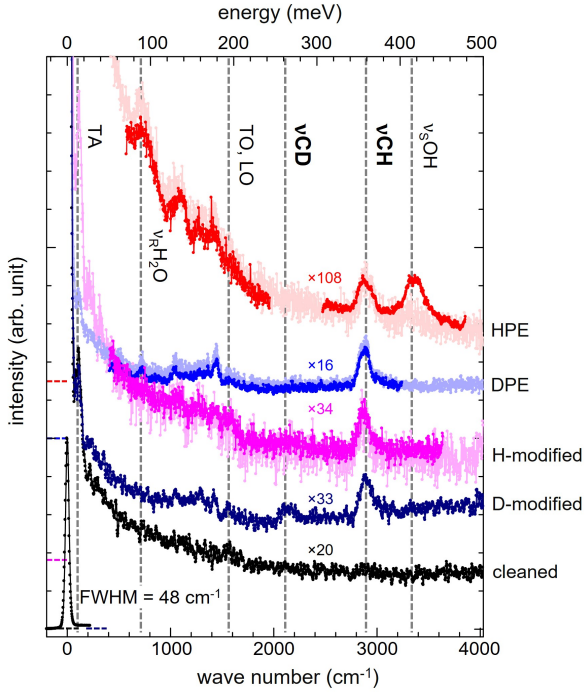


Figure 3: HREELS spectra for the HPE, DPE, H-modified, D-modified and cleaned samples from top to bottom. The detection angle is 50° for the HPE, DPE and D-modified samples, while it is 45° for the other samples. The spectra are shifted for clarity, and the horizontal dotted lines indicate the offset. The vertical dotted lines show the energy losses of each vibration; ν_{SOH} and $\nu_{\text{RH}_2\text{O}}$ are H_2O -related oscillations, while TA, LO and TO are the graphite surface phonon modes. ν_{CH} and ν_{CD} are the C-H and C-D stretching modes, respectively.

D-modified sample, another isolated peak is also observed at 2143 cm^{-1} . These two peaks at higher energies around 2890 cm^{-1} and at 2143 cm^{-1} can be the stretching modes. Considering that two of the samples, the H- and the D-modified samples, are prepared in-situ in UHV, these stretching modes can be related to the vibrations of the edge atoms rather than unknown contamination. Since the energy ratio of these two peaks, which is about 1.35, is comparable to the one between ν_{CH} and ν_{CD} for edges of the graphene nanoislands on Pt surfaces [21, 22] and for submonolayer benzene [23] and cyclohexane [24] on Pt(111), and is also comparable to the square root of the mass ratio between H and D, one can assign the peaks at around 2890 cm^{-1} and 2143 cm^{-1} to the ν_{CH} and ν_{CD} , respectively.

Here, the ν_{CD} appears weaker than the ν_{CH} for the D-modified sample and is even missing for the

DPE sample. This can be related to our sample preparation conditions. In the D-modified sample, the ν_{CD} appears weaker than the ν_{CH} probably because D atoms stick on a graphite edge less than do H atoms, which are generated from the residual H_2 gas in the UHV chamber. The mass spectrum in the UHV chamber indicates that the H_2 exist about 1% of the D_2 amount during the process. In fact, the sticking probability of H atoms on graphite surface is calculated to be higher than that of D atoms at the sample preparation conditions in this study [30], namely the H and D atoms are thermally dissociated at $T \sim 1700\text{ K}$ and are exposed to graphite at $T \sim 100\text{ K}$. It may also be the case on graphite edge. For the DPE sample, on the other hand, the ν_{CD} is missing probably because the D-plasma does not create hexagonal nanopits efficiently under the sample preparation conditions in this study. Indeed, as discussed above, the anisotropic etching effect of the D-plasma is weaker than or similar to that of the H-plasma. Therefore, the plasma of the residual H_2 gas in the etching chamber rather than the D-plasma probably anisotropically etches the surface more efficiently under these etching conditions. Note that the DPE sample is prepared in a chamber for the plasma etching which is made of a glass tube and evacuated by a rotary pump to $P \sim 0.4\text{ Pa}$. This implies that more H_2 gas remains in the etching chamber than in the UHV chamber for HREELS. However, further studies are desired to confirm these hypotheses and to fully understand these behaviors.

In any case, it is confirmed unambiguously that the edges are terminated by H and/or D atoms. To identify edge bonding, either sp^2 or sp^3 , we compare the stretching modes with previous measurements for graphene nanoislands [21, 22], the counterstructure to the sample in this study, the nanopits. The ν_{CH} at the edges of graphene nanoislands appeared at 2700 cm^{-1} on Pt(111) and at 2675 cm^{-1} on Pt(100), while the ν_{CD} was observed at 1990 cm^{-1} on Pt(111) and at 1940 cm^{-1} on Pt(100), which are significantly lower than those observed in this measurement. Since the difference between the nanopits and the nanoislands is too large to explain by the difference in the structure and substrate, the bonding condition can be different between them. Considering that the stretching mode for sp^2 bonding appears at around 100 cm^{-1} higher energy than that for sp^3 bonding [23, 24], it can be expected that the stretching mode for the graphene nanopit (this study) is sp^2 bonding, while that for the graphene nanoisland (previous study) is sp^3 bonding. It should be noted

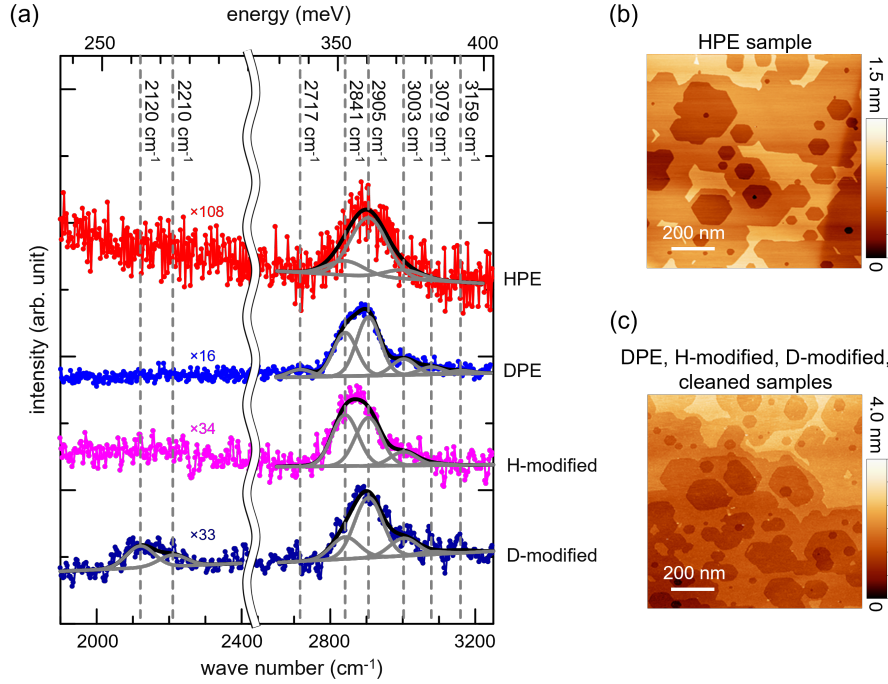


Figure 4: (a) Gaussian fitting of ν_{CH} and ν_{CD} peaks. Each gaussian position and the number of gaussians are determined using sparse modeling. Each gaussian is shown in gray curves, while the sum of the component is shown in black. (b,c) Typical topographic images of (b) the HPE sample and (c) the DPE, H-modified, D-modified and cleaned samples. (b) is obtained on graphite which is etched by H-plasma simultaneously with the HPE sample for the HREELS. On the other hand, (c) is exactly the surface studied by HREELS.

that, although the energies of ν_{CH} and ν_{CD} of the nanopits coincide with those of submonolayer cyclohexane, i.e., sp^3 bonding, on metallic substrates [24, 31], the assumption that the edge bonding of the nanopits is sp^3 is unlikely because the bonding of the edge of the nanoisland cannot be assigned if this is the case. In addition, it is also difficult to expect that the edge bonding of a flat graphene shows the same energy within 10 cm^{-1} as that of cyclohexane, the benzene ring of which has a steric structure.

Moreover, the ν_{CH} observed in this measurement at around 2890 cm^{-1} agrees very well with the calculations of the local vibrational density of states for graphene nanoribbons with sp^2 -bonded edges, in which the ν_{CH} is calculated at around 2900 cm^{-1} [25, 26]. This again suggests that the edges created by H-plasma etching are sp^2 bonded and terminated by only one H atom. It is interesting to note that a bunch of peaks also appeared in these calculations similarly to our measurement.

Although the peaks at around 2890 cm^{-1} and 2143 cm^{-1} originate from the ν_{CH} and ν_{CD} of sp^2 -bonded edges, respectively, one can find that the peak is not a simple gaussian but contains detailed structure. Therefore, each spectral peak is decomposed into several components by assuming that the

peak is the sum of several gaussian peaks with the same FWHM ($\sim 50 \text{ cm}^{-1}$ for the HPE sample and $\sim 35 \text{ cm}^{-1}$ for the other samples) as shown in Figure 4(a). The peak position and the number of peaks are determined using the LASSO (least absolute shrinkage and selection operator) technique of sparse modeling. It is found that the ν_{CH} consists of four components, while the ν_{CD} consists of two components. The fact that the stretching mode peak is composed of several gaussian peaks is possibly due to the imperfection of the edges and a somewhat complicated surface structure, since the vibrational energy loss can be shifted easily for about 50 cm^{-1} by the different interaction with surrounding atoms [21, 22] and the displacement of H atoms from their equilibrium position [26]. Therefore, although it is difficult to identify the origin of each component, it can be assumed that the two main components of ν_{CH} at 2841 cm^{-1} and 2905 cm^{-1} are related to the corner and the straight edge of the hexagonal nanopit, respectively. Indeed, the ratio of the straight edge component at 2905 cm^{-1} is larger among the other components for the HPE sample than the DPE sample, because the hexagonal nanopits are larger and have longer straight edges for the HPE sample than the DPE sample as can be seen in the STM images

(Figure 4(b,c)).

4. SUMMARY

In this study, the differences between H- and D-plasma etching of graphite are studied by STM, and termination of the edges created by H- and D-plasma etching are studied by HREELS. To avoid uncontrollable conditions such as surface contamination during the transfer of the sample from the etching chamber to the UHV chamber for HREELS, four kinds of graphite surfaces are studied throughout this measurement. These are H- and D-plasma etched surfaces, and surfaces with H- and D-modified edges. The last two samples are prepared based on the DPE sample in-situ in the UHV chamber for HREELS.

All the samples show a complicated peak structure at lower energies than 1600 cm^{-1} and isolated peaks at around 2890 cm^{-1} and 2143 cm^{-1} in HREELS spectra. The isolated peaks are related to the νCH and νCD , suggesting that the edges are terminated by H and/or D atoms. By comparing the stretching mode with previous studies on graphene nanoislands and theoretical calculations for graphene nanoribbons, it can be concluded that the edge created by H-plasma etching is sp^2 bonded and the edge C atom is terminated by only one H atom. From

the STM study of the etching behavior by H- and D-plasma together with this HREELS measurement, it is also found that D-plasma hardly etches graphite anisotropically although it can make defects more efficiently than H-plasma. It is good to note, too, that the edge termination is robust even in air, since the C-H and C-D vibrations at edges can be observed by HREELS even after transferring the sample from the etching chamber to the UHV chamber. From this study together with previous STM/S studies [32], it can be concluded that not only atomically precise but also sp^2 -bonded zigzag edges can be obtained by the H-plasma etching of graphite and graphene. Thus, this sample preparation technique provides an opportunity to study the exotic properties of graphene zigzag edges such as a spin-polarized zigzag edge state.

Acknowledgments

HREELS measurement was carried out by the joint research between Anritsu Corporation and The Institute for Solid State Physics, The University of Tokyo. The authors acknowledge the free-to-use software, WSxM[33] and Imaje-J Fiji[34].

-
- [1] K. S. Novoselov, A. K. Geim, S. V. Morozov, D. Jiang, Y. Zhang, S. V. Dubonos, et al., Electric Field Effect in Atomically Thin Carbon Films, *Science* 306 (2004) 666–669.
 - [2] K. S. Novoselov, A. K. Geim, S. V. Morozov, D. Jiang, M. I. Katsnelson, I. V. Grigorieva, et al., Two-dimensional gas of massless Dirac fermions in graphene, *Nature* 438 (7065) (2005) 197–200.
 - [3] Y. Zhang, Y.-W. Tan, H. L. Stormer, P. Kim, Experimental observation of the quantum Hall effect and Berry's phase in graphene, *Nature* 438 (7065) (2005) 201–204.
 - [4] Y. Cao, V. Fatemi, S. Fang, K. Watanabe, T. Taniguchi, E. Kaxiras, P. Jarillo-Herrero, Unconventional superconductivity in magic-angle graphene superlattices, *Nature* 556 (7699) (2018) 43–50.
 - [5] H. Toyama, R. Akiyama, S. Ichinokura, M. Hashizume, T. Iimori, Y. Endo, et al., Two-Dimensional Superconductivity of Ca-Intercalated Graphene on SiC: Vital Role of the Interface between Monolayer Graphene and the Substrate, *ACS nano* 16 (3) (2022) 3582–3592.
 - [6] H. Zhou, T. Xie, T. Taniguchi, K. Watanabe, A. F. Young, Superconductivity in rhombohedral trilayer graphene, *Nature* 598 (7881) (2021) 434–438.
 - [7] M. Yankowitz, Q. Ma, P. Jarillo-Herrero, B. J. LeRoy, van der Waals heterostructures combining graphene and hexagonal boron nitride, *Nature Reviews Physics* 1 (2) (2019) 112–125.
 - [8] J. Liu, S. Bao, X. Wang, Applications of Graphene-Based Materials in Sensors: A Review, *Micromachines* 13 (2) (2022) 184.
 - [9] Y. Ronen, T. Werkmeister, D. Haie Najafabadi, A. T. Pierce, L. E. Anderson, Y. J. Shin, et al., Aharonov–Bohm effect in graphene-based Fabry–Pérot quantum Hall interferometers, *Nature nanotechnology* 16 (5) (2021) 563–569.
 - [10] C. Déprez, L. Veyrat, H. Vignaud, G. Nayak, K. Watanabe, T. Taniguchi, et al., A tunable fabry–pérot quantum Hall interferometer in graphene, *Nature nanotechnology* 16 (5) (2021) 555–562.

- [11] M. Fujita, K. Wakabayashi, K. Nakada, K. Kusakabe, Peculiar localized state at zigzag graphite edge, *Journal of the Physical Society of Japan* 65 (7) (1996) 1920–1923.
- [12] Y. Kobayashi, K.-i. Fukui, T. Enoki, K. Kusakabe, Y. Kaburagi, Observation of zigzag and armchair edges of graphite using scanning tunneling microscopy and spectroscopy, *Phys. Rev. B* 71 (2005) 193406–193409.
- [13] Y. Niimi, T. Matsui, H. Kambara, K. Tagami, M. Tsukada, H. Fukuyama, Scanning tunneling microscopy and spectroscopy studies of graphite edges, *Applied Surface Science* 241 (1-2) (2005) 43–48.
- [14] Y. Niimi, T. Matsui, H. Kambara, K. Tagami, M. Tsukada, H. Fukuyama, Scanning tunneling microscopy and spectroscopy of the electronic local density of states of graphite surfaces near monoatomic step edges, *Phys. Rev. B* 73 (2006) 085421–8.
- [15] R. Yang, L. Zhang, Y. Wang, Z. Shi, D. Shi, H. Gao, et al., An anisotropic etching effect in the graphene basal plane, *Advanced Materials* 22 (36) (2010) 4014–4019.
- [16] G. Diankov, M. Neumann, D. Goldhaber-Gordon, Extreme monolayer-selectivity of hydrogen-plasma reactions with graphene, *ACS Nano* 7 (2) (2013) 1324–1332.
- [17] D. Hug, S. Zihlmann, M. K. Rehm, Y. B. Kalyoncu, T. N. Camenzind, L. Marot, et al., Anisotropic etching of graphite and graphene in a remote hydrogen plasma, *npj 2D Materials and Applications* 1 (1) (2017) 1–6.
- [18] T. Matsui, H. Sato, K. Kita, A. E. Amend, H. Fukuyama, Hexagonal nanopits with the zigzag edge state on graphite surfaces synthesized by hydrogen-plasma etching, *The Journal of Physical Chemistry C* 123 (36) (2019) 22665–22673.
- [19] T. Yokosawa, M. Kamada, T. Ochi, Y. Koga, R. Takehara, M. Hara, et al., Nanoscale Fabrication of Graphene by Hydrogen-Plasma Etching, *e-Journal of Surface Science and Nanotechnology* 20 (3) (2022) 139–144.
- [20] X. Zhang, O. V. Yazyev, J. Feng, L. Xie, C. Tao, Y.-C. Chen, et al., Experimentally engineering the edge termination of graphene nanoribbons, *ACS Nano* 7 (1) (2013) 198–202.
- [21] T. Zecho, A. Horn, J. Biener, J. Küppers, Hydrogen atom reactions with monolayer graphite edges on Pt(100) surfaces: hydrogenation and H abstraction, *Surface Science* 397 (1-3) (1998) 108–115.
- [22] A. Dinger, C. Lutterloh, J. Biener, J. Küppers, Hydrogen atom reactions with graphite island edges on Pt(111) surfaces: hydrogenation through Eley-Rideal and hot-atom processes, *Surface Science* 421 (1-2) (1999) 17–26.
- [23] S. Lehwald, H. Ibach, J. Demuth, Vibration spectroscopy of benzene adsorbed on Pt(111) and Ni(111), *Surface Science* 78 (3) (1978) 577–590.
- [24] D. P. Land, W. Erley, H. Ibach, HREELS investigation of the orientation and dehydrogenation of cyclohexane on Pt[111], *Surface Science* 289 (3) (1993) 237–246.
- [25] M. Vandescuren, P. Hermet, V. Meunier, L. Henrard, P. Lambin, Theoretical study of the vibrational edge modes in graphene nanoribbons, *Physical Review B* 78 (19) (2008) 195401–8.
- [26] M. S. Islam, S. Tanaka, A. Hashimoto, Effect of vacancy defects on phonon properties of hydrogen passivated graphene nanoribbons, *Carbon* 80 (2014) 146–154.
- [27] D. Chakarov, L. Österlund, B. Kasemo, Water adsorption on graphite(0001), *Vacuum* 46 (8-10) (1995) 1109–1112.
- [28] L. Wirtz, A. Rubio, The phonon dispersion of graphite revisited, *Solid State Communications* 131 (3-4) (2004) 141–152.
- [29] A. Allouche, Y. Ferro, T. Angot, C. Thomas, J.-M. Layet, Hydrogen adsorption on graphite(0001) surface: A combined spectroscopy–density-functional-theory study, *The Journal of Chemical Physics* 123 (12) (2005) 124701–6.
- [30] S. Morisset, Y. Ferro, A. Allouche, Isotopic effects in the sticking of H and D atoms on the(0 0 0 1) graphite surface, *Chemical Physics Letters* 477 (1-3) (2009) 225–229.
- [31] J. E. Demuth, H. Ibach, S. Lehwald, CH Vibration Softening and the Dehydrogenation of Hydrocarbon Molecules on Ni(111) and Pt(111), *Phys. Rev. Lett.* 40 (1978) 1044–1047.
- [32] A. E. Amend, T. Matsui, H. Sato, H. Fukuyama, STS Studies of Zigzag Graphene Edges Produced by Hydrogen-Plasma Etching, *e-Journal of Surface Science and Nanotechnology* 16 (2018) 72–75.
- [33] I. Horcas, R. Fernández, J. Gomez-Rodriguez, J. Colchero, J. Gómez-Herrero, A. Baro, WSXM: A software for scanning probe microscopy and a tool for nanotechnology, *Review of Scientific Instruments* 78 (1) (2007) 013705–8.
- [34] J. Schindelin, I. Arganda-Carreras, E. Frise, V. Kaynig, M. Longair, T. Pietzsch, et al., Fiji: an

open-source platform for biological-image analysis,
Nature Methods 9 (7) (2012) 676–682.

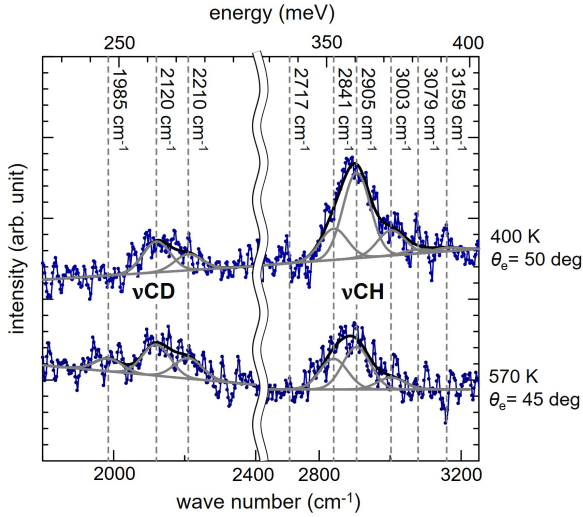


Figure S1: HREELS spectra for the D-modified sample after annealing at $T = 400$ K (upper) and 570 K (lower). The detection angle (θ_e) are 50° and 45° , respectively. The spectral peaks are decomposed into several gaussian peaks using a sparse modeling technique.

5. SUPPLEMENTARY

5.1. Effect of the sample annealing

The effect of the sample annealing is studied for the D-modified sample. The spectra around the ν CH

and the ν CD after the annealing at $T = 400$ K and 570 K are shown in Figure S1. It is found that the edge termination is robust up to $T = 400$ K. Intuitively, just the peak intensity decreases as the edge terminating H/D atoms are removed by increasing the anneal temperature. However, when it is annealed at $T = 570$ K, not only the peak intensity but also the peak structure are modified. Therefore, each peak is decomposed into several gaussian peaks using a sparse modeling technique (The details are the same as written in the main text).

For the ν CH, only the peak intensity at 2905 cm^{-1} decreases by annealing at $T = 570$ K. Considering that the elemental peak at 2905 cm^{-1} is related to the ν CH on the straight edge of nanopit, while the elemental peak at 2841 cm^{-1} is related to the one at the corner edge, this result suggests that the edge termination along the straight edge might be easier to be removed by heating than the termination at the corner edge.

For the ν CD, on the other hand, an additional peak appears at 1985 cm^{-1} . Interestingly, this peak energy coincides with the stretching mode of sp^3 -bonded C-D at the graphene nanoisland edge on Pt surfaces [21, 22]. Therefore, this fact implies that the edge termination changes from sp^2 to sp^3 by annealing.